Published in final edited form as:
J Nat Prod. 2010 June 25; 73(6): 1080–1086. doi:10.1021/np100087c.

Fijiolides A and B, Inhibitors of TNF-α Induced NFκB Activation, from a Marine-Derived Sediment Bacterium of the Genus *Nocardiopsis*

Sang-Jip Nam[†], **Susana P. Gaudêncio**[†], **Christopher A. Kauffman**[†], **Paul R. Jensen**[†], **Tamara P. Kondratyuk**[‡], **Laura E. Marler**[‡], **John M. Pezzuto**[‡], and **William Fenical**[*,†]

[†]Center for Marine Biotechnology and Biomedicine, Scripps Institution of Oceanography, University of California-San Diego, La Jolla, CA 92093-0204

[‡]College of Pharmacy, University of Hawaii at Hilo, Hilo, Hawaii 96720

Abstract

Fijiolide A, a potent inhibitor of TNF-α induced NFκB activation, along with fijiolide B, were isolated from a marine-derived bacterium of the genus *Nocardiopsis*. The planar structures of fijiolides A (**1**) and B (**2**) were elucidated by interpretation of 2D NMR spectroscopic data, while the absolute configurations of these compounds were defined by interpretation of circular dichroism (CD) and 2D NMR data combined with application of the advanced Mosher's method. Fijiolides A and B are related to several recently isolated chloroaromatic compounds, which appear to be the Bergman cyclization products of enediyne precursors. Fijiolide A reduced TNF-α induced NFκB activation by 70.3%, with an IC_{50} value of 0.57 μM. Fijiolide B demonstrated less inhibition, only 46.5%, without dose-dependence. The same pattern was also observed with quinone reductase (QR) activity: fijiolide A was found to induce quinone reductase-1 (QR1), with an induction ratio (IR) of 3.5 at a concentration of 20 μg/mL (28.4 μM). The concentration required to double activity (CD) was 1.8 μM. Fijiolide B did not affect QR1 activity, indicating the importance of the nitrogen substitution pattern for biological activity. Based on these data, fijiolide A is viewed as a promising lead for more advanced anticancer testing.

Nature is an important resource for the discovery of anticancer drugs. The relevance of the marine environment as a source of novel anticancer compounds has been validated by discovery ca. 2,500 new metabolites with antiproliferative activity.1 Bacteria belonging to the order *Actinomycetales*, commonly known as actinomycetes, have provided nearly 50% of the bioactive microbial natural products discovered as of 2002.2 Although most microbial small molecule discovery efforts have focused on actinomycetes from terrestrial environments, marine-derived actinomycetes are proving to be an important resource that has led to the discovery of biologically active molecules with unique chemical structures.3 Excellent examples are the salinosporamides4a and marinomycins.4b Salinosporamide A, isolated from *Salinispora tropica*, is a potent 20S proteasome inhibitor that recently completed phase I clinical trials for treatment of solid tumors, lymphomas, and multiple myeloma. The marinomycins isolated from a "*Marinispora*" sp. showed significant antimicrobial activity against drug-resistant bacterial pathogens and selective cancer cell cytotoxicity against melanoma cell lines.4b

Corresponding Author: Tel: 1-858-534-2133; Fax: 1-858-534-1318; wfenical@ucsd.edu.

Supporting Information Available: The ^{1}H, ^{13}C, and 2D NMR spectra of fijiolide A (**1**) and ^{1}H spectrum of fijiolide B (**2**), and ^{1}H NMR spectrum of MTPA esters **3a**, **3b**, **4a**, **4b**, **6a**, **6b**, and ^{1}H NMR spectrum of acetonide **5** are available free of charge via the Internet at http://pubs.acs.org.

As part of a program to explore marine bacterial metabolites as inhibitors of tumor initiation and promotion, we have targeted nuclear factor kappa B (NFκB), a transcription factor that regulates the expression of more than 400 different genes. NFκB is an inducible, well-characterized protein, responsible for the regulation of complex phenomena, with a pivotal role in controlling cell signaling.5 Many genes activated by NFκB encode proteins that are involved in tumorigenesis, including cyclooxygenase (COX)-2 and matrix metalloproteinase (MMP)-9, adhesion molecules, chemokines, inflammatory cytokines, inducible nitric oxide synthase (iNOS), and antiapoptosis proteins bcl-2 and bcl-xl.6 Constitutive expression of NFκB is a frequent occurrence in tumor cells, and inhibitors of NFκB have the potential of suppressing carcinogenesis.7 Since NFκB represents an important and attractive therapeutic target for drugs to treat many disorders, including arthritis, asthma, auto-immune diseases, as well as different types of cancer, it has become a focal point for drug discovery from different sources, including the marine environment. Over the last decade, several compounds have been discovered that selectively interfere with the NFκB pathway. Examples include phenols and polyphenols (e.g., curcumin, resveratrol, caffeic acid phenethyl ester, quercetin, epigallocatechin-3-gallate), lignans, sesquiterpenes, diterpenes, and triterpenes.8 The majority of these compounds are antioxidants, which act by blocking the protein kinase-mediated IκB degradation thereby preventing NFκB activation.

An additional strategy for protecting cells from cancer initiation involves decreasing metabolic enzymes responsible for generating reactive species (phase I enzymes) while increasing phase II enzymes that can deactivate radicals and electrophiles known to intercede in normal cellular processes. Reduction of electrophilic quinones by quinone reductase (QR) is an important detoxification pathway, and induction of this enzyme often correlates with induction of other phase II enzymes such as glutathione *S*-transferase. Based on the evaluation of approximately 3,800 marine organism extracts, the percentage characterized as “active” QR activators was established in the range of 17% of the total. About 60 QR inducers have been isolated from a diversity of sources, and substantial molecular diversity has been observed. These active compounds comprise ceramides, terpenoids, withanolides, flavonoids, chalcones, alkaloids, and diarylheptanoids.8

As part of our collaborative program to define new modulators of NFκB and QR, the marine-derived actinomycete strain CNS-653, isolated from a marine sediment sample collected from the Beqa Lagoon, Fiji, was evaluated. Analysis of the 16S rRNA gene sequence places this strain within the genus *Nocardiopsis* (GQ374440). Strain CNS-653 shares a nearly identical (99.8%) 16S sequence with another marine-derived strain, CNR-712 (EF392847), which produces the modified peptides lucentamycins A-D, and was isolated from a marine sediment sample collected in the Bahamas.9 LCMS analysis of a whole culture extract of this strain revealed peaks illustrating the characteristic MS isotopic patterns of dichlorinated secondary metabolites ($[M+H]^+$:$[M+H+2]^+$:$[M+H+4]^+$ = 10:6:1). Fractionation of a 30 L culture extract of this strain by standard silica column chromatography, followed by reversed-phase HPLC separation, yielded fijiolides A (**1**, 31.0 mg) and B (**2**, 3.0 mg) as colorless non-crystalline solids. Herein, we report details of the isolation and structure elucidation of fijiolides A and B, and their effects on TNF-α induced NFκB activity and QR induction.

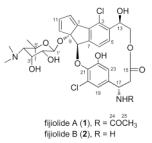

The molecular formula of **1** was deduced as $C_{34}H_{39}Cl_2N_2O_{10}$, based on analysis of HRESIMS data (a pseudomolecular ion peak at *m/z* 705.1997 $[M+H]^+$) and on interpretation

of ^{13}C NMR data. The ^{1}H NMR spectrum of **1** displayed *ortho*-coupled aromatic protons [δ_H 7.08 (d, *J* = 8.0 Hz), 6.64 (d, *J* = 8.0 Hz)], *meta*-coupled aromatic protons [δ_H 6.52 (d, *J* = 2.0 Hz), 5.98 (d, *J* = 2.0 Hz)], three olefinic protons [δ_H 6.76 (d, *J* = 2.1 Hz), 6.65 (dd, *J* = 5.3, 2.1 Hz), 6.62 (d, *J* = 5.3 Hz)], and three downfield methine protons [δ_H 5.87 (s), 4.66 (dd, *J* = 11.0, 4.0 Hz), 4.61 (ddd, *J* = 13.4, 13.4, 3.8 Hz)]. The ^{1}H NMR and ^{13}C NMR spectra also revealed two *N*-methyl groups [δ_H 2.79 (δ_C 44.4 and 42.9)], three methyl singlets [δ_H 1.46 (δ_C 20.6), δ_H 1.43 (δ_C 31.5), δ_H 1.70 (δ_C 22.6)], and six exchangeable protons [(4-OH, 2-NH); δ_H 9.09, 8.45, 8.41, 5.86, 5.73, 4.95]. Interpretation of 2D NMR spectoscopic data allowed three partial structures to be constructed: a benzodihydropentalene, a 3′-chloro-5′-hydroxy-β-tyrosine, and an aminosugar unit. COSY NMR data, including crosspeaks from H-11 (δ_H 6.65, dd, *J* = 5.3, 2.1 Hz) to H-10 (δ_H 6.62, d, *J* = 5.3 Hz) and H-12 (δ_H 6.76, d, *J* = 2.1 Hz), along with the 1D proton coupling constants of these three protons, indicated that they belonged to a cyclopentadienyl spin system. The presence of *ortho*-coupled aromatic protons [H-5 (δ_H 6.64, d, *J* = 8.0 Hz) and H-6 (δ_H 7.08, d, *J* = 8.0 Hz)] indicated a 1, 2, 3, 4-tetrasubstituted benzene ring. The connection between the cyclopentadienyl moiety and the 1, 2, 3, 4-tetrasubstituted benzene ring was established by long-range HMBC correlations observed from H-12 (δ_H 6.76) to C-1 (δ_C 148.8), C-2 (δ_C 135.7), C-9 (δ_C 99.8), and C-10 (δ_C 135.5); from H-8 (δ_H 5.87) to C-1 (δ_C 148.8), C-2 (δ_C 135.7), C-6 (δ_C 125.3), C-7 (δ_C 147.7), C-9 (δ_C 99.8), and C-10 (δ_C 135.5); and from H-6 (δ_H 7.08) to C-2 (δ_C 135.7), C-7 (δ_C 147.7), and C-8 (δ_C 83.2). The oxygenated methine proton H-13 (δ_H 4.66), which was coupled to the methylene protons H_2-14 (δ_H 4.23, and δ_H 3.64), also displayed long-range HMBC correlations to carbons C-3 (δ_C 126.7), C-4 (δ_C 139.3), and C-5 (δ_C 129.1). These data allowed construction of the benzodihydropentalene unit in **1** (C-1 to C-12).

The 3′-chloro-5′-hydroxy-β-tyrosine amino acid component was established by the observation of COSY NMR crosspeaks between a downfield methine proton H-17 (δ_H 4.61) and the methylene protons H_2-16 (δ_H 2.57, and δ_H 2.07)]. In addition, these assignments were also confirmed by long-range HMBC NMR correlations from H-17 to C-15 (δ_C 170.0), C-18 (δ_C 138.8), C-19 (δ_C 114.2), C-23 (δ_C 113.9), and C-24 (δ_C 168.4), and from the phenol proton 22-OH (δ_H 8.45) to C-21 (δ_C 138.3), C-22 (δ_C 151.0), and C-23 (δ_C 113.9). The connection between C-8 and C-21 was established by a three-bond HMBC correlation from H-8 (δ_H 5.87) to C-21 (δ_C 138.3).

The 4-deoxy-4-dimethylamino-5,5-dimethyl-ribopyranose sugar was constructed based upon analysis of COSY and HMBC NMR spectroscopic data. COSY NMR correlations permitted construction of the spin system from the anomeric proton H-1′ through H-4′ [H1′ (δ_H 4.45, d, *J* = 8.0 Hz)-H-2′ (δ_H 2.92, dd, *J* = 8.0, 3.4 Hz)- H-3′ (δ_H 4.06, d, *J* = 8.0, 3.4 Hz)- H-4′ (δ_H 2.98)] of the aminosugar. Long-range HMBC correlations from the *N*-dimethyl protons (δ_H 2.79) to C-4′ (δ_C 69.6) and from the dimethyl protons (δ_H 1.46, 1.43) to C-4′ (δ_C 69.6), and C-5′ (δ_C 75.0) allowed placement of these protons at C-4′ and C-5′, respectively. A long-range HMBC correlation from the anomeric proton H-1′ (δ_H 4.45) to C-9 (δ_C 99.8) provided evidence for placing the sugar at C-9. The three-bond HMBC correlations from the methylene protons H-14 (δ_H 4.23, 3.64) to the carbonyl carbon C-15 (δ_C 170.0) and from the methine proton H-17 (δ_H 4.61) to the carbonyl carbon C-24 (δ_C 168.4) permitted the ester linkage between C-14 and C-15, and the amide linkage between C-17 and C-24, respectively. Lastly, placement of the chlorine at C-3 completed the structure assignment of **1**.

The molecular formula of **2** was assigned as $C_{32}H_{36}{}^{35}Cl_2N_2O_9$, based upon the pseudomolecular ion peak at *m/z* 663.1871 $[M+H]^+$ observed in the HRESIMS spectrum. The ^{1}H NMR spectrum of **2** was almost identical to that of **1** except for an up-field shifted methine proton H-17 (δ_H 4.09) and the absence of one methyl singlet. This difference

indicated **2** possessed a primary amine at C-17 instead of an acetamide group. Interpretation of 2D COSY, HSQC, and HMBC NMR spectroscopic data allowed the planar structure of **2** to be assigned as shown.

The relative and absolute configurations of **1** and **2** were determined by analysis of CD spectroscopic data, application of the advanced Mosher's method, and by combined spectroscopic methods. Fijiolides A (**1**) and B (**2**) were assigned identical absolute configurations based upon the virtually identical CD curves observed for these two metabolites (Figure 1).

The relative configuration of the ribopyranose ring of **1** was determined by analysis of vicinal coupling constants and by analysis of NOESY spectroscopic data. The magnitude of the $^{1}J_{CH}$ coupling constant for the anomeric proton (H-1′, 162 Hz) indicated that this center possesses a β-configuration.10 A large diaxial coupling constant (8.0 Hz) between H-1′ and H-2′ indicated an axial configuration for H-2′, while a small vicinal coupling constant (3.4 Hz) between H-2′ and H-3′ and strong NOESY correlations between H-2′ and H-3′ and between H-3′ and H-4′ established that H-2′ and H-3′ are in the equatorial and axial positions, respectively (Figure 2). Determination of the absolute configuration of the ribopyranose of **1** was achieved using the advanced Mosher method involving NMR analysis of MTPA ester pairs produced by derivatization with (*R*)- and (*S*)- MTPACl (α-methoxy-α-(trifluoromethyl) phenylacetyl chloride).11 Calculation of $\Delta\delta_{S-R}$ values of *bis*-MTPA esters (**3a**/**b**) clearly established the absolute configuration of C-2′ as *R* and allowed the absolute configuration of the ribopyranose to be assigned as 1′*S*, 2′*R*, 3′*R*, 4′*S* (Figure 3a).

The absolute configurations at C-17 and C-13 in **1** and **2** were determined as *S* and *R*, respectively, also by the application of the advanced Mosher's method. Treatment of **2** in pyridine *R*-(−)-MTPA-Cl and (*S*)-(+)- MTPA-Cl yielded the MTPA amides **4a** and **4b**. Positive $\Delta\delta_{S-R}$ values for H-19 and H-23, and negative $\Delta\delta_{S-R}$ values for H_2-16 allowed the absolute configuration of C-17 to be assigned as *S* (Figure 3b). To assign the absolute configurations at C-13, the 1, 2-diol groups of the ribopyranose in **1** were first protected by conversion to the acetonide **5** using 2,2-dimethoxypropane and pyridinium *p*-toluenesulfate in methanol (Scheme 1). Treatment of **5** in pyridine with *R*-MTPA-Cl and *S*-MTPA-Cl yielded the *S*-MTPA ester **6a** and *R*-MTPA ester **6b**, respectively. Calculation of $\Delta\delta_{S-R}$ values of MTPA esters of **6a**/**b** established the absolute configuration of C-13 as *R* (Figure 3c).

The absolute configurations of the remaining components of **1** were determined by interpretation of NOESY NMR correlations. A NOESY correlation between H-8 (δ_H 5.87) and the anomeric proton H-1′ (δ_H 4.45) of the ribopyranose suggested a *trans*-orientation of the C-9 glycoside and C-8 ether bonds.12 There were the only two possible stereoisomers, (8*R*, 9*R*) or (8*S*, 9*S*), for fijiolides as shown in Figure 4. A NOESY correlation between H-12 and 22-OH revealed that ester and ether linkages between the two aromatic rings of **1** restrict free rotation of the β-tyrosine moiety in fijiolides (Figure 4a/b). The strong NOESY correlations, between H-5 and H-13, and between H-17 and H-23, suggeste that C-8 and C-9 could be assigned *R*, and *R* configurations, respectively (Figure 4a).13

The chloro-cyclopenta[*a*]indene carbon skeleton of the fijiolides resembles that of the cyanosporasides14a and sporolides,14b isolated from strains of the marine actinomycete genus *Salinispora* (Figure 5). Both cyanosporasides A and B (**7**/**8**) and sporolides A and B (**9**/**10**) are equally represented in the respective fermentation extracts of the producing strains. This is what would be expected for the cycloaromatization of the enediyne precursors to Bergman diradical intermediates followed by nonspecific quenching with

hydrogen15a or chloride, a process that has been experimentally verified.15b Interestingly, chloride addition occurred primarily at the C-3 position in fijiolides A and B. Energy minimized modeling of fijiolides revealed that C-6 in the benzene ring is in closer proximity to the chlorine atom of β-tyrosine than C-3 is to the 22-OH group of β-tyrosine (Figure 6). The ribopyranose is also located near C-6 in the fijiolides, further restricting chloride addition to that site.

With the exception of the chlorine substituents, the fijiolides are nearly identical to the aromatization product from the bacterial metabolite C-1027 chromophore (**11**), derived from an antitumor antibiotic enediyne, C-1027 (**12**), isolated in 1988 by Marunaka *et al*. from the culture broth of *Streptomyces globisporus*.16 C-1027 is responsible for the activity of the complete C-1027 natural product, which consists of an apo-protein with a single polypeptide chain of 110 amino acid residues and a chromophore with the nine-membered enediyne and benzoxazine moieties. In 1995, Yu *et al.* demonstrated that loss of the benzoxazine moiety in the aromatization product of C-1027 resulted in a substantial decrease of DNA binding affinity (~400 fold).17 Fijiolides A and B, which resemble the aromatization product of C-1027 chromophore without its benzoxazine moiety, do not display significant activity against either HCT-116 or methicillin-resistant *Stapyhlococcus aureus* (MRSA) (data not shown).

NFκB plays a central role in a variety of disease states, including cancer. As a transcription factor, activated NFκB regulates the expression of numerous genes, which subsequently influence cell survival, proliferation, differentiation, and inflammation.18,19 Numerous studies demonstrating the effects of different compounds on NFκB activity have been reported. However, the results of these studies are often inconsistent, which is likely due to the use of diverse cell types and assay methods. For assessment of NFκB activity, we used stably transfected 293 human embryonic kidney cells that demonstrated NFκB activation by treatment with 12-*O*-tetradecanoylphorbol-13-acetate, as well as TNF-α. We observed a 5 to 15-fold NFκB activation by treatment with 0.14 nM TNF-α, high values for luciferase luminescence, and good reproducibility.20 With this assay, fijiolide A inhibited TNF-α induced NFκB activity by 70.3%, and dose-dependence demonstrated an IC_{50} value of 0.57 μM. Fijiolide B was less active, showing only 46.5% without a dose-dependent response.

An established mechanism of cancer chemoprevention involves the stimulation of metabolic detoxification activity. The detoxification enzyme quinone reductase 1 (QR1) is an important phase II enzyme (one that deactivates reactive and potentially carcinogenic species) which converts quinones to hydroquinones, reducing oxidative cycling.21 The enzyme exhibits broad specificity, reducing a wide range of hydrophobic quinones of varying structure.22 The induction of QR often coincides with induction of other phase II enzymes, and is therefore useful in the study of chemopreventive agents. Hepa 1c1c7 (mouse hepatoma) cells were used to assess quinone reductase activity via a color change as MTT is reduced to a blue formazan.23 Fijiolide A (**1**) was found to enhance QR1 activity with an induction ratio (IR) of 3.5 at 20 μg/mL (28.4 μM). The concentration required to double induction (CD) was 1.8 μM (The CD value of 4-bromoflavone, as a positive control, is 0.013 μM). Fijiolide B did not demonstrate QR1 induction activity, indicating that substitutions on the nitrogen atom affect activity. Differential activity of this type was also observed with the NFκB assay.

QR1 is well established to undergo transcriptional activation through NFκB signaling pathways.24 Although NFκB alone seems to account for only 20–30% of QR promoter activity, revealed by mutational analysis, NFκB is responsible for a proportion of the immediate response of the QR gene promoter.25 Significant inhibition of luciferase NFκB activity and QR activation was detected with fijiolide A at reasonably low concentrations

(IC_{50} for NFκB, 0.57 μM; CD for QR1, 1.8 μM). It is likely that QR activation is NFκB independent. In summary, fijiolide A modulates distinct and important mechanisms, and this would be worthy of more detailed investigation.

General Experimental Procedures

The optical rotations were measured using a Rudolph Research Autopol III polarimeter with a 10-cm cell. UV spectra were recorded in a Varian Cary UV-visible spectrophotometer with a path length of 1 cm and IR spectra were recorded on a Perkin-Elmer 1600 FTIR spectrometer. CD spectra were collected in an AVIV model 215 CD spectrometer with a 0.5 cm long cell. ^{1}H and 2D NMR spectra data were recorded at 500 or 600 MHz in DMSO-d_6, $CDCl_3$, or methanol-d_4 solution containing Me_4Si as internal standard on Varian Inova spectrometers. ^{13}C NMR spectra were acquired at 150 MHz on a Varian Inova spectrometer. High resolution ESI-TOF mass spectra were provided by The Scripps Research Institute, La Jolla, CA or by the mass spectrometry facility at the Department of Chemistry and Biochemistry at the University of California, San Diego, La Jolla, CA. Low resolution LC/MS data were measured using a Hewlett-Packard series 1100 LC/MS system with a reversed-phase C_{18} column (Phenomenex Luna, 4.6 mm × 100 mm, 5 μm) at a flow rate of 0.7 mL/min.

Collection and Phylogenetic Analysis of Strain CNS-653

The marine-derived actinomycete, strain CNS-653, was isolated from a surf zone sediment sample collected near Beqa Island in Beqa Lagoon in Fiji, July 2006. NCBI BLAST analysis of the partial 16S rDNA sequence of CNQ-653 (deposited with GenBank as accession number GQ374440) indicates that this strain is affiliated with the genus *Nocardiopsis*.

Cultivation and Extraction

The bacterium (strain CNS-653) was cultured in 30 2.8 L Fernbach flasks each containing 1 L of a seawater-based medium (10 g starch, 4 g yeast extract, 2 g peptone, 1 g $CaCO_3$, 40 mg $Fe_2(SO_4)_3$•$4H_2O$, 100 mg KBr) and shaken at 230 rpm at 27 °C. After seven days of cultivation, sterilized XAD-16 resin (20 g/L) was added to adsorb the organic products, and the culture and resin were shaken at 215 rpm for 2 h. The resin was filtered through cheesecloth, washed with deionized water, and eluted with acetone. The acetone was removed under reduced pressure, and the resulting aqueous layer was extracted with EtOAc (3 × 500 mL). The EtOAc-soluble fraction was dried *in vacuo* to yield 3.5 g of extract.

Isolation of Fijiolides A and B

The extract (3.5 g) was fractionated by open column chromatography on silica gel (25 g), eluted with a step gradient of CH_2Cl_2 and MeOH. The CH_2Cl_2/MeOH 5:1 fraction contained a mixture of both fijiolides, which were purified by reversed-phase HPLC (Phenomenex Ultracarb C30, 250 × 100 mm, 2.0 ml/min, 5 μm, 100 Å, UV = 210 nm) using a gradient solvent system from 5% to 100% CH_3CN (0.05% TFA) over 60 min to afford fijiolides A (**1**, 30.0 mg) and B (**2**, 3.0 mg), as pale yellow oils.

Fijiolide A (1)

pale yellow oil; $[\alpha]_D^{21}$ −440 (*c* 0.5, MeOH); UV (MeOH) λ_{max} (logε) 213 (4.4), 285 (3.7), 330 (2.7) nm; IR (KBr) ν_{max} 3380, 1725, 1677, 1512, 1190, 1128 cm^{-1}; ^{1}H and 2D-NMR (600 MHz, DMSO-d_6), see Table 1; HRESIMS $[M + H]^+$ *m*/*z* 705.1997 (calcd for $C_{34}H_{39}O_{10}N_2Cl_2$, 705.1976).

Fijiolide B (2)

pale yellow oil; $[\alpha]_D^{21}$ −360 (*c* 0.2, MeOH); UV (MeOH) λ_{max} (logε) 213 (4.3), 285 (3.8), 330 (2.7) nm; IR (KBr) ν_{max} 3383, 1678, 1512, 1201, 1134, 1048 cm^{-1}; ^1H and 2D-NMR (600 MHz, DMSO-d_6), see Table 2; HRESITOFMS $[M + H]^+$ *m/z* 663.1871 (calcd for $C_{32}H_{37}O_9N_2Cl_2$, 663.1871).

Bis-MTPA Esters of 1 (3a/3b)

Fijiolide A (7.0 mg) was dissolved in freshly distilled dry pyridine (2 mL) and several dry crystals of dimethylaminopyridine were added. The mixture was stirred for 15 min at RT. Treatment with *R*-(-)-MTPA-Cl yielded the *bis*-*S*-MTPA ester at 60 °C after 12 h. The reaction was quenched by 1 mL of MeOH. After removal of solvent under vacuum, the residue was purified by reversed-phase HPLC (Phenomenex Luna 5*u* C18 (2) 100 Å, 250 × 100 mm, 2.0 ml/min, UV detection (at 210 nm) using a gradient solvent system from 5% to 100 % CH_3CN (0.05% TFA) over 50 min. The *bis*-*S*-MTPA ester was obtained at 36 min. The *bis*-*R*-MTPA ester was prepared with *S*-MTPA-Cl in the same manner. $\Delta\delta_{S-R}$ values for the *S*- and *R*-MTPA esters of **1** were recorded in ppm in methanol-d_4.

Bis-*S*-MTPA Ester of Fijiolide A (3a)

^1H NMR (600 MHz, methanol-d_4): δ 7.55 (m, 2H), 7.45-7.30 (m, 8H), 6.89 (d, 1H, *J* = 1.5 Hz), 6.63 (d, 1H, *J* = 5.9 Hz), 6.589 (dd, 1H, *J* = 5.9, 3.0 Hz), 6.484 (d, 1H, *J* = 8.0 Hz), 6.42 (d, 1H, *J* = 3.0 Hz), 6.292 (d, 1H, *J* = 8.0 Hz), 5.802 (dd, 1H, *J* = 11.0, 4.0 Hz), 5.54 (s, 1H), 4.717 (d, 1H, *J* = 11.0 Hz), 4.69 (dd, 1H, *J* = 11.0, 4.0 Hz), 4.678 (dd, 1H, *J* = 11.0, 4.0 Hz), 4.465 (t, 1H, *J* = 11.0 Hz), 4.39 (t, 1H, *J* = 1.2 Hz), 3.71 (s, 1H), 3.646 (dd, 1H, *J* = 11.0, 4.0 Hz), 3.37 (s, 3H), 3.270 (d, 1H, *J* = 2.0 Hz), 2.910 (s, 6H), 2.60 (t, 1H, *J* = 11.0 Hz), 2.55 (s, 3H), 2.14 (t, 1H, *J* = 11.0 Hz), 1.822 (s, 3H), 1.449 (s, 3H), 1.443 (s, 3H); ESI-MS *m/z* 1137 $[M+H]^+$, ESI-MS *m/z* 1159 $[M+Na]^+$.

Bis-*R*-MTPA Ester of Fijiolide A (3b)

^1H NMR (600 MHz, methanol-d_4): δ 7.74 -7.30 (m, 12H), 7.021 (d, 1H, *J* = 8.0 Hz), 6.83 (d, 1H, *J* = 1.5 Hz), 6.736 (d, 1H, *J* = 8.0 Hz), 6.67 (d, 1H, *J* = 5.9 Hz), 6.59 (dd, 1H, *J* = 5.9, 3.0 Hz), 5.86 (s, 1H), 5.856 (dd, 1H, *J* = 11.0, 4.0 Hz), 4.857 (d, 1H, *J* = 11.0 Hz), 4.72 (dd, 1H, *J* = 11.0, 4.0 Hz), 4.680 (dd, 1H, *J* = 11.0, 4.0 Hz), 4.492 (t, 1H, *J* = 11.0 Hz), 4.376 (t, 1H, *J* = 1.2 Hz), 3.864 (dd, 1H, *J* = 11.0, 4.0 Hz), 3.52 (s, 3H), 3.263 (d, 1H, *J* = 1.2 Hz), 2.95 (s, 3H), 2.899 (s, 6H), 2.62 (t, 1H, *J* = 11.0 Hz), 2.20 (t, 1H, *J* = 11.0 Hz), 1.822 (s, 3H), 1.499 (s, 3H), 1.493 (s, 3H); ESI-MS *m/z* 1137 $[M+H]^+$, ESI-MS *m/z* 1159 $[M+Na]^+$.

MTPA Amides of 2 (4a/4b)

Fijiolide B (1.3 mg) was dissolved in freshly distilled dry pyridine (2 mL), several dry crystals of dimethylaminopyridine were added, and the mixture was stirred for 15 min at RT. Treatment with *R*-(-)-MTPA-Cl yielded the *S*-MTPA amide at room temperature after 11 h. The reaction was quenched by 1 mL of MeOH. After removal of solvent under vacuum, the residue was purified by reversed-phase HPLC (Phenomenex Luna 5*u* C18 (2) 100 Å, 250 × 100 mm, 2.0 ml/min, UV detection at 210 nm) using a gradient solvent system from 5% to 100% CH_3CN (0.05% TFA) over 60 min. The *S*-MTPA amide was obtained at 41 min. The *R*-MTPA amide was prepared with *S*-MTPACl in the same manner. Δδ*S*-*R* values for the *S*- and *R*-MTPA amides of **2** were recorded in ppm in DMSO-d_6.

S-MTPA Amide of Fijiolide B (4a)

^{1}H NMR (600 MHz, DMSO-d_6) δ 9.96 (d, 1H, *J* = 7.4 Hz), 8.98 (br s, 1H), 7.36-7.25 (m, 5H), 7.08 (d, 2H, *J* = 8.0 Hz), 6.738 (m, 1H), 6.64-6.59 (m, 4H), 6.040 (m, 1H), 6.03 (m, 1H), 5.89 (m, 1H), 5.80 (m, 1H), 4.99 (m, 1H), 4.73 (m, 1H), 4.640 (m, 1H), 4.48 (d, 1H, *J* = 10.0 Hz), 4.27 (dd, 1H, *J* = 10.4, 10.4 Hz), 4.06 (m, 1H), 3.78 (s, 3H), 3.62 (dd, 1H, *J* = 11.0, 6.0 Hz), 3.00 (s, 6H), 2.92 (br s, 1H), 2.91 (m, 1H), 2.840 (m, 1H), 2.110 (dd, 1H, *J* = 11.0, 2.0 Hz), 1.37 (br s, 6H); ESI-MS *m/z* 879 $[M+H]^+$, ESI-MS *m/z* 901 $[M+Na]^+$.

R-MTPA Amide of Fijiolide B (4b)

^{1}H NMR (600 MHz, DMSO-d_6) δ 8.98 (br s, 1H), 8.91 (d, 1H, *J* = 7.4 Hz), 7.36-7.25 (m, 5H), 7.17 (d, 2H, *J* = 8.0 Hz), 6.718 (m, 1H), 6.711 (d, 1H, *J* = 2.0), 6.67-6.62 (m, 3H), 6.10 (d, 1H, *J* = 2.0), 6.020 (m, 1H), 5.87 (m, 1H), 5.77 (m, 1H), 4.99 (m, 1H), 4.68 (m, 1H), 4.644 (m, 1H), 4.46 (d, 1H, *J* = 10.0 Hz), 4.24 (dd, 1H, *J* = 10.4, 10.4 Hz), 4.06 (m, 1H), 3.82 (s, 3H), 3.64 (dd, 1H, *J* = 11.0, 6.0 Hz), 2.92 (br s, 1H), 2.91 (m, 1H), 2.79 (s, 6H), 2.841 (m, 1H), 2.116 (dd, 1H, *J* = 11.0, 2.0 Hz), 1.40 (br s, 6H); ESI-MS *m/z* 879 $[M+H]^+$, ESI-MS *m/z* 901 $[M+Na]^+$.

Acetonide 5

Fijiolide A (**1**, 5.0 mg) was dissolved in 4 mL of dry MeOH solution, along with 5 mg of pyridinium-*p*-toluenesulfonate and 5 mg of *p*-toluenesulfonic acid. The solution was cooled in an ice water bath and 2 mL of 2,2-dimethoxypropane was added. The solution was stirred at 60 °C for 12 h. The reaction was quenched with 5% aq. $NaHCO_3$ and the product was extracted with EtOAc. The EtOAc was removed *in vacuo* and the residual material was purified by reversed-phase HPLC (Phenomenex Ultracarb C30 100 Å, 250 × 100 mm, 2.0 ml/min, UV detection at 210 nm) using a gradient solvent system from 5% to 100 % CH_3CN (0.05% TFA) over 60 min. The acetonide **5** (4.8 mg) was isolated with a retention time of 31 min.

For Acetonide 5

^{1}H NMR (500 MHz, methanol-d_4) δ 7.35 (d, 1H, *J* = 8.0 Hz), 6.99 (d, 1H, *J* = 1.5 Hz), 6.82 (dd, 1H, *J* = 5.8, 3.0 Hz), 6.78 (d, 1H, *J* = 5.8 Hz), 6.59 (d, 1H, *J* = 3.0 Hz), 6.15 (d, 1H, *J* = 1.5 Hz), 5.94 (s, 1H), 4.83 (m, 2H), 4.65 (m, 1H), 4.55 (dd, 1H, *J* = 10.4, 10.4 Hz), 4.31 (d, 1H, *J* = 11.0 Hz), 3.79 (dd, 1H, *J* = 10.4, 3.5 Hz), 3.62 (t, 1H, *J* = 3.5 Hz), 3.55 (m, 1H), 3.44 (m, 1H), 3.04 (br s, 6H), 2.72 (dd, 1H, *J* = 12.4, 2.8 Hz), 2.26 (t, 1H, *J* = 12.4 Hz), 1.93 (s, 3H), 1.60 (s, 3H), 1.54 (s, 3H), 1.35 (s, 3H), 1.21 (s, 3H); ESI-MS *m/z* 745 $[M+H]^+$, ESI-MS *m/z* 767 $[M+Na]^+$.

MTPA Esters of 5 (6a/6b)

The acetonide **5** (2.4 mg) was dissolved in freshly distilled dry pyridine (2 ml) and several dry crystals of dimethylaminopyridine were added. The mixture was stirred for 15 min at RT. Treatment with *R*-(-)-MTPA-Cl yielded the *S*-MTPA ester at room temperature after 11 h. The reaction was quenched by 1 mL of methanol. After removal of solvent under vacuum, the residue was purified by reversed-phase HPLC (Phenomenex Luna 5*u* C18 (2) 100 Å, 250 × 100 mm, 2.0 ml/min, UV detection at 210 nm) using a gradient solvent system from 5% to 100 % CH_3CN (0.05% TFA) over 40 min. The *S*-MTPA ester was eluted at 30 min. The *R*-MTPA ester prepared with *S*-MTPA-Cl in the same manner. $\Delta\delta_{S-R}$ values for the *S*- and *R*-MTPA esters of acetonides were recorded in ppm in $CDCl_3$.

S-MTPA Ester of Acetonide 5 (6a)

^{1}H NMR (600 MHz, $CDCl_3$) δ 7.428 (d, 1H, *J* = 8.0 Hz), 7.390 (d, 1H, *J* = 8.0 Hz), 7.34-7.28 (m, 5H), 6.93 (s, 1H), 6.85 (d, 1H, *J* = 8.0 Hz), 6.79 (s, 1H), 6.40 (s, 1H), 6.20 (d, 1H, *J* = 2.0 Hz) 5.855 (dd, 1H, *J* = 12.1, 4.0 Hz), 5.73 (m, 1H), 4.85 (m, 1H), 4.605 (t, 1H, *J* = 12.1 Hz), 4.48 (d, 1H, *J* = 2.0 Hz), 4.16 (d, 1H, *J* = 11.0 Hz), 3.774 (dd, 1H, *J* = 11.0, 4.0 Hz), 3.47 (m, 1H), 3.43 (s, 3H), 3.27 (m,1H), 2.90 (m, 2H), 2.85 (s, 6H), 2.11 (t, 1H, *J* = 11.0 Hz), 1.91 (s, 3H), 1.56 (s, 3H), 1.51 (s, 3H), 1.18 (s, 3H), 1.07 (s, 3H); ESI-MS *m/z* 961 $[M+H]^+$, ESI-MS *m/z* 983 $[M+Na]^+$.

R-MTPA Ester of Acetonide 5 (6b)

^{1}H NMR (600 MHz, $CDCl_3$) δ 7.428 (d, 1H, *J* = 8.0 Hz), 7.390 (d, 1H, *J* = 8.0 Hz), 7.34-7.28 (m, 5H), 6.90 (s, 1H), 6.84 (d, 1H, *J* = 8.0 Hz), 6.79 (s, 1H), 6.40 (s, 1H), 6.20 (d, 1H, *J* = 2.0 Hz) 5.845 (dd, 1H, *J* = 12.1, 4.0 Hz), 5.70 (m, 1H), 4.85 (m, 1H), 4.660 (t, 1H, *J* = 12.1 Hz), 4.46 (d, 1H, *J* = 2.0 Hz), 4.15 (d, 1H, *J* = 11.0 Hz), 3.884 (dd, 1H, *J* = 11.0, 4.0 Hz), 3.47 (m, 1H), 3.44 (s, 3H), 3.27 (m,1H), 2.90 (m, 2H), 2.87 (s, 6H), 2.12 (t, 1H, *J* = 11.0 Hz), 1.91 (s, 3H), 1.61 (s, 3H), 1.51 (s, 3H), 1.18 (s, 3H), 1.07 (s, 3H); ESI-MS *m/z* 961 [M+H]+, ESI-MS *m/z* 983 $[M+Na]^+$.

NFκ B Assay

Panomics Inc. (Fremont, CA) has established NFκB reporter stable cells in a number of popular cell lines suitable for specific applications in the study of NFκB. We employed human embryonic kidney cells 293 (Panomics Inc.; Fremont, CA) for monitoring any changes occurring along the NFκB pathway. Stably transfected cells were seeded into sterile 96-well plates at a density of 20×10^3 cells per well. Cells were maintained in Dulbecco's modified Eagle's medium (DMEM) (Invitrogen, Carlsbad, CA), supplemented with 10% FBS, 100 units/mL penicillin, 100 μg/mL streptomycin, and 2 mM L-glutamine. After an incubation period of 48 h, the medium was replaced and various concentrations of test chemicals (dissolved in PBS) were added. Human recombinant TNF-α (Calbiochem, Gibbstown, NJ) was used as an activator (2 ng/mL). Following a 6 h incubation period, the medium was discarded and the cells were washed once with PBS. The cells were then lysed by adding 50 μL/well (diluted with water 5 times) of Reporter Lysis Buffer (Promega, Madison, WI), and incubating for 5 min with shaking. The plates were then stored at −80 °C until the luciferase assay was performed using the Luc assay system from Promega.20 The gene product, luciferase enzyme, reacts with luciferase substrate, emitting light which was detected in a luminometer (LUMIstar Galaxy BMG). Data are expressed as IC_{50} values (i.e., concentration required to inhibit TNF-α activated NFκB activity by 50%).

Quinone Reductase 1 (QR1) Assay

QR1 activity was assessed in 96-well plates using Hepa 1c1c7 murine hepatoma cells as previously described.26 Briefly, cells were grown to a density of 2×10^4 cells/mL in 200 μL of MEM-α containing 5% antibiotic-antimycotic (Gibco) and 10% fetal bovine serum at 37 °C in 5% CO_2 atmosphere. After preincubation for 24 h, the media was changed and test compounds were added to a final concentration of 20 μg/mL. For dose-dependence, samples were added in five serial three-fold dilutions, starting at 20 μg/mL. The cells were incubated with test samples for an additional 48 h. Quinone reductase activity was measured as a function of the NADPH-dependent menadiol-mediated reduction of 3-(4,5-dimetylthiazo-2-yl)-2,5-diphenyltetrazolium bromide (MTT) to a blue formazan.23 Cytotoxicity was determined via crystal violet staining of identical plates. Specific activity is defined as nmol of formazan formed per mg protein per min.27 The induction ratio (IR) of QR activity represents the specific enzyme activity of agent-treated cells compared with a DMSO-

treated control. The concentration to double activity (CD) was determined through a dose-response assay for active substances (IR >2).

Supplementary Material

Refer to Web version on PubMed Central for supplementary material.

Acknowledgments

Financial support was provided by the National Cancer Institute, NIH (under grant P01 CA048112) and U01-TW007401-O1, the latter under the Fogerty Center's International Cooperative Biodiversity Groups program. We thank the people of Fiji in the Beqa Lagoon region and W. Aalbersberg (University of the South Pacific) for providing laboratory space and facilitating field collections. We also thank the government of Fiji for permission to export samples and work in their territorial waters. S.P.G. is grateful to the Fundação para a Ciência e Tecnologia, Portugal, for a postdoctoral fellowship. We thank Dr. C. C. Hughes for his generous advice in the determination of the configurations of fijiolides A and B.

References and Notes

1. Jimeno J, Faircloth G, Fernandez Sousa-Faro JM, Scheuer P, Rinehart K. Mar. Drugs. 2004; 2:14–29.
2. Bérdy J. J. Antibiot. 2005; 58:1–26. [PubMed: 15813176]
3. (a) Hughes CC, MacMillan JB, Gaudêncio SP, Fenical W, La Clair JJ. Angew. Chem., Int. Ed. Engl. 2009; 48:728–732. [PubMed: 19097126] (b) Hughes CC, MacMillan JB, Gaudêncio SP, Jensen PR, Fenical W. Angew. Chem., Int. Ed. Engl. 2009; 48:725–727. [PubMed: 19090514] (c) Huang S-X, Zhao L-X, Tang S-K, Jiang C-L, Duan Y, Shen B. Org. Lett. 2009; 11:1353–1356. [PubMed: 19228040] (d) Sato S, Iwata F, Mukai T, Yamada S, Takeo J, Abe A, Kawahara H. J. Org. Chem. 2009; 74:5502–5509. [PubMed: 19572603] (e) Raju R, Piggott AM, Conte M, Aalbersberg WGL, Feussner K, Capon RJ. Org. Lett. 2009; 11:3862–3865. [PubMed: 19655766] (f) Schneider K, Keller S, Wolter FE, Röglin L;W, Beil W, Seitz O, Nicholson G, Bruntner C, Riedlinger J, Fiedler H-P, Süssmuth RD. Angew. Chem., Int. Ed. Engl. 2008; 47:3258–3261. [PubMed: 18348121] (g) Boonlarppradab C, Kauffman CA, Jensen PR, Fenical W. Org. Lett. 2008; 10:5505–5508. [PubMed: 19007176] (h) Hughes CC, Prieto-Davo A, Jensen PR, Fenical W. Org. Lett. 2008; 10:629–631. [PubMed: 18205372] (i) Oh D-C, Strangman WK, Kauffman CA, Jensen PR, Fenical W. Org. Lett. 2007; 9:1525–1528. [PubMed: 17373804] (j) Fenical W, Jensen PR. Nat. Chem. Biol. 2006; 2:666–673. and references therein. [PubMed: 17108984]
4. (a) Feling RH, Buchanan GO, Mincer TJ, Kauffman CA, Jensen PR, Fenical W. Angew. Chem., Int. Ed. 2003; 42:355–357. (b) Kwon HC, Kauffman CA, Jensen PR, Fenical W. J. Am. Chem. Soc. 2006; 128:1622–1632. [PubMed: 16448135]
5. Bode AM, Dong Z. Mutation Res. 2004; 555:33–51. [PubMed: 15476850]
6. (a) Aggarwal BB, Sethi G, Nair A, Ichikawa H. Curr. Signal Transduction Ther. 2006; 1:25–52. (b) Melisi D, Chiao PJ. Expert Opin. Ther. Targets. 2007; 11:133–144. [PubMed: 17227230] (c) Kim HJ, Hawke N, Baldwin AS. Cell Death Differ. 2006; 13:738–747. [PubMed: 16485028] (d) Pikarsky E, Ben-Neriah Y. Eur. J. Cancer. 2006; 42:779–784. [PubMed: 16530406]
7. (a) Inoue J, Gohda J, Akiyama T, Semba K. Cancer Sci. 2007; 98:268–274. [PubMed: 17270016] (b) Shen H-M, Tergaonkar V. Apoptosis. 2009; 14:348–363. [PubMed: 19212815]
8. Nguyen-Hai N. Mini-Rev. Med. Chem. 2006; 6:945–951. [PubMed: 16918500]
9. Cho JY, Williams PG, Kwon HC, Jensen PR, Fenical W. J. Nat. Prod. 2007; 70:1321–1328. [PubMed: 17630797]
10. The typical ranges of $^{1}J_{CH}$ values are 169–171 and 158–162 Hz for α- and β-linkages, respectively ($^{1}J_{CH}$ value was measured from the $^{1}J_{CH}$ satellites in the gHMBC experiment). See: Pretsch, E.; Bühlmann, P.; Affolter, C. Structure Determination of Organic Compounds-Tables of Spectral Data. New York: Springer; 2000. p. 153
11. (a) Ohtani I, Kusumi T, Kashman Y, Kakisawa H. J. Am. Chem. Soc. 1991; 113:4092–4096. (b) Seco JM, Quinoa E, Riguera R. Chem. Rev. 2004; 104:12–117.

12. (a) Minami Y, Yoshida K, Azuma R, Saeki M, Otani T. Tetrahedron Lett. 1993; 34:2633–2636. (b) Yoshida K, Minami Y, Azuma R, Saeki M, Otani T. Tetrahedron Lett. 1993; 34:2637–2640.
13. Iida K, Fukuda S, Tanaka T, Hirama M. Tetrahedron Lett. 1996; 37:4997–5000.
14. (a) Oh D-C, Williams PG, Kauffman CA, Jensen PR, Fenical W. Org. Lett. 2006; 8:1021–1024. [PubMed: 16524258] (b) Buchanan GO, Williams PG, Feling RH, Kauffman CA, Jensen PR, Fenical W. Org. Lett. 2005; 7:2731–2733. [PubMed: 15957933]
15. (a) Bharucha KN, Marsh RM, Minto RE, Bergman RG. J. Am. Chem. Soc. 1992; 114:3120–3121. (b) Perrin CL, Rodgers BL, O'Connor JM. J. Am. Chem. Soc. 2007; 129:4795–4799. [PubMed: 17378569]
16. (a) Hu J, Xue Y-C, Xie M-Y, Zhang R, Otani T, Minami Y, Yamada Y, Marunaka T. J. Antibiot. 1988; 41:1575–1579. [PubMed: 3198491] (b) Otani T, Minami Y, Marunaka T, Zhang R, Xie M-Y. J. Antibiot. 1988; 41:1580–1585. [PubMed: 3198492]
17. Yu L, Mah S, Otani T, Dedon P. J. Am. Chem. Soc. 1995; 117:8877–8878.
18. Tergaonkar V. Intern. J. Biochem. Cell Biol. 2006; 38:1647–1653.
19. Ghosh S, Karin M. Cell. 2002; 109:S81–S96. [PubMed: 11983155]
20. Homhual S, Bunyapraphatsara N, Kondratyuk T, Herunsalee A, Chaukul W, Pezzuto JM, Fong HHS, Zhang HJ. J. Nat. Prod. 2006; 69:421–424. [PubMed: 16562850]
21. Cuendet M, Oteham CP, Moon RC, Pezzuto JM. J. Nat. Prod. 2006; 69:460–463. [PubMed: 16562858]
22. Su B-N, Gu J-Q, Kang Y-H, Park EJ, Pezzuto JM, Kinghorn AD. Mini-Rev. Org. Chem. 2004; 1:115–123.
23. Kennelly EJ, Gerhäuser C, Song LL, Graham JG, Beecher CWW, Pezzuto JM, Kinghorn AD. J. Agric. Food Chem. 1997; 45:3771–3777.
24. Yao KS, O'Dwyer PJ. Biochem. Pharmacol. 2003; 66:15–23. [PubMed: 12818361]
25. Nho CW, O'Dwyer PJ. J. Biol. Chem. 2004; 279:26019–26027. [PubMed: 15047705]
26. Song LL, Kosmeder JW II, Lee SK, Gerhäuser C, Lantvit D, Moon RC, Moriarty RM, Pezzuto JM. Cancer Res. 1999; 59:578–585. [PubMed: 9973203]
27. Gerhauser C, You M, Liu J, Moriarty RM, Hawthorne M, Mehta RG, Moon RC, Pezzuto JM. Cancer Res. 1997; 57:272–278. [PubMed: 9000567]

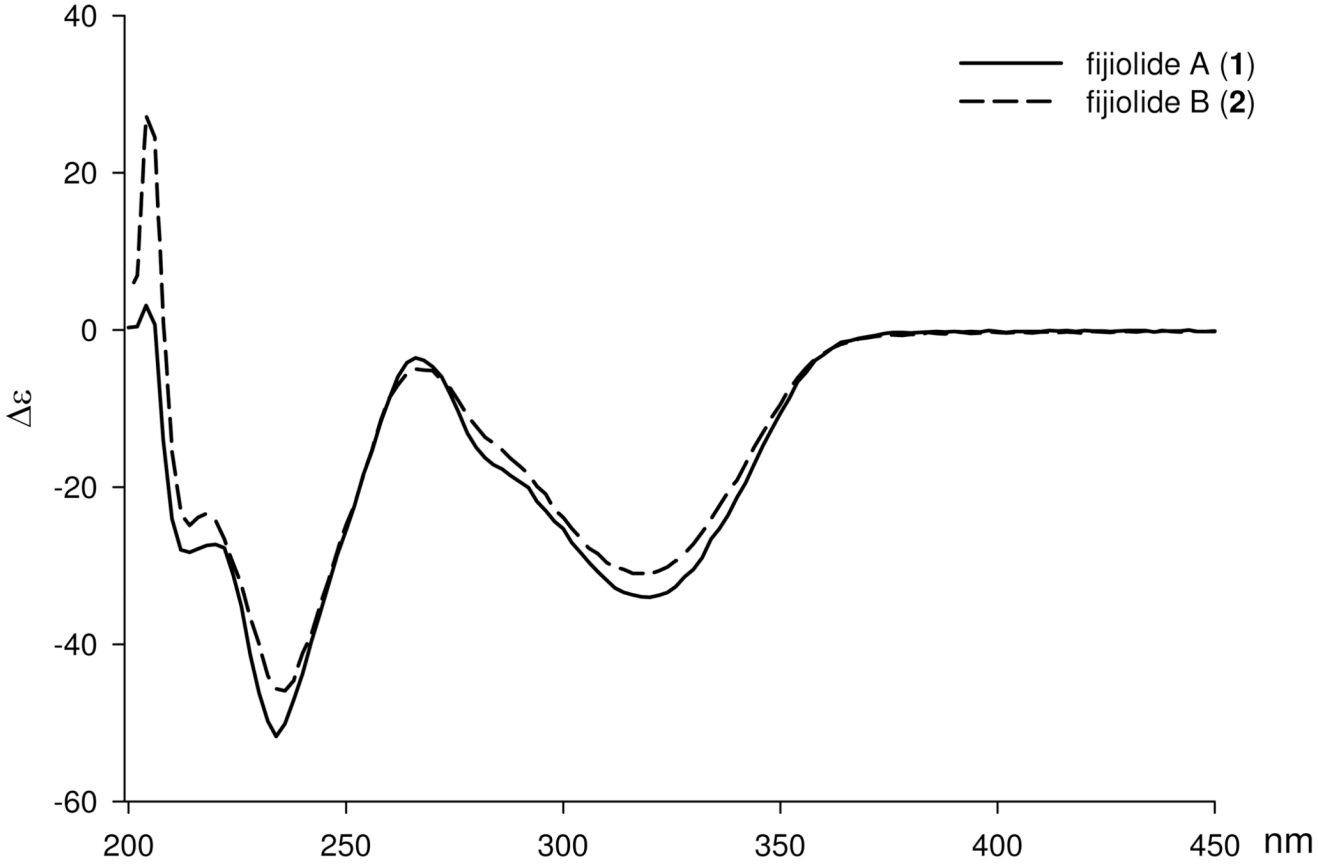

Figure 1.
CD spectra for fijiolides A (**1**) and B (**2**) in MeOH (7.1e-4 M)

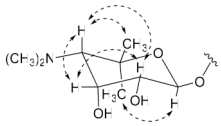

Figure 2.
Relative configuration of the ribopyranose based on key NOESY correlations (Dashed arrows).

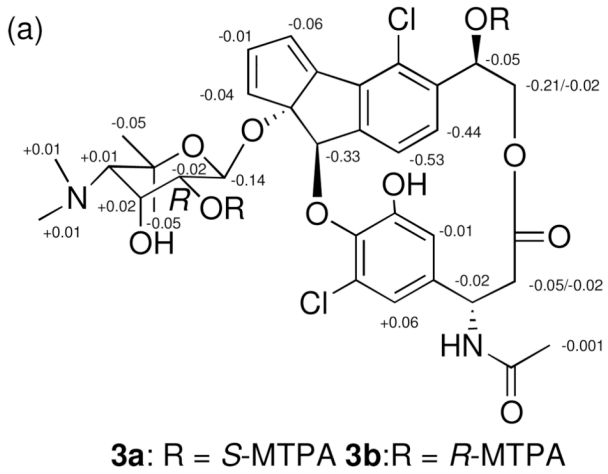

3a: R = *S*-MTPA **3b**:R = *R*-MTPA

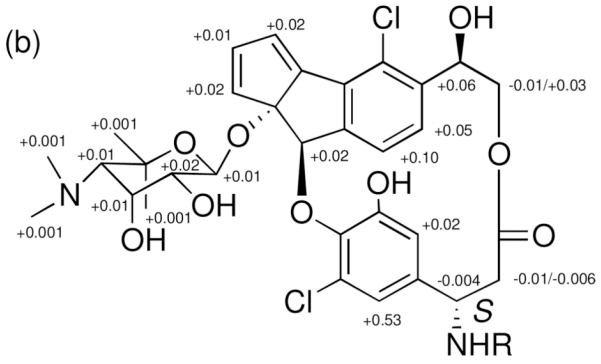

4a: R = *S*-MTPA **4b**: R = *R*-MTPA

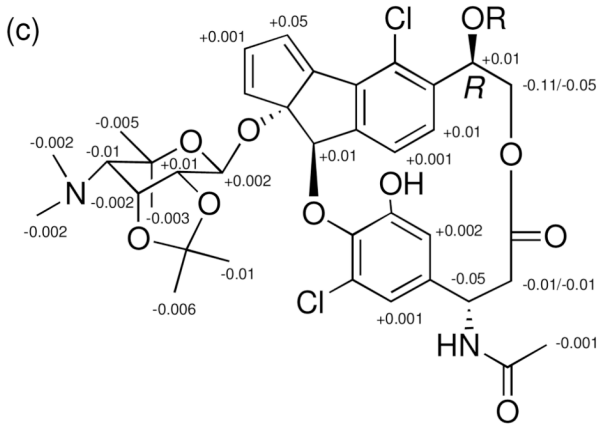

6a: R = *S*-MTPA **6b**: R = *R*-MTPA

Figure 3.

$\Delta\delta_{S-R}$ of ^{1}H for *S*- and *R-bis*-MTPA esters of **1** (a), $\Delta\delta_{S-R}$ of ^{1}H for *S*- and *R*-mono-MTPA amides of **2** (b), $\Delta\delta_{S-R}$ of ^{1}H for *S*- and *R*-mono-MTPA esters of **1** (c).

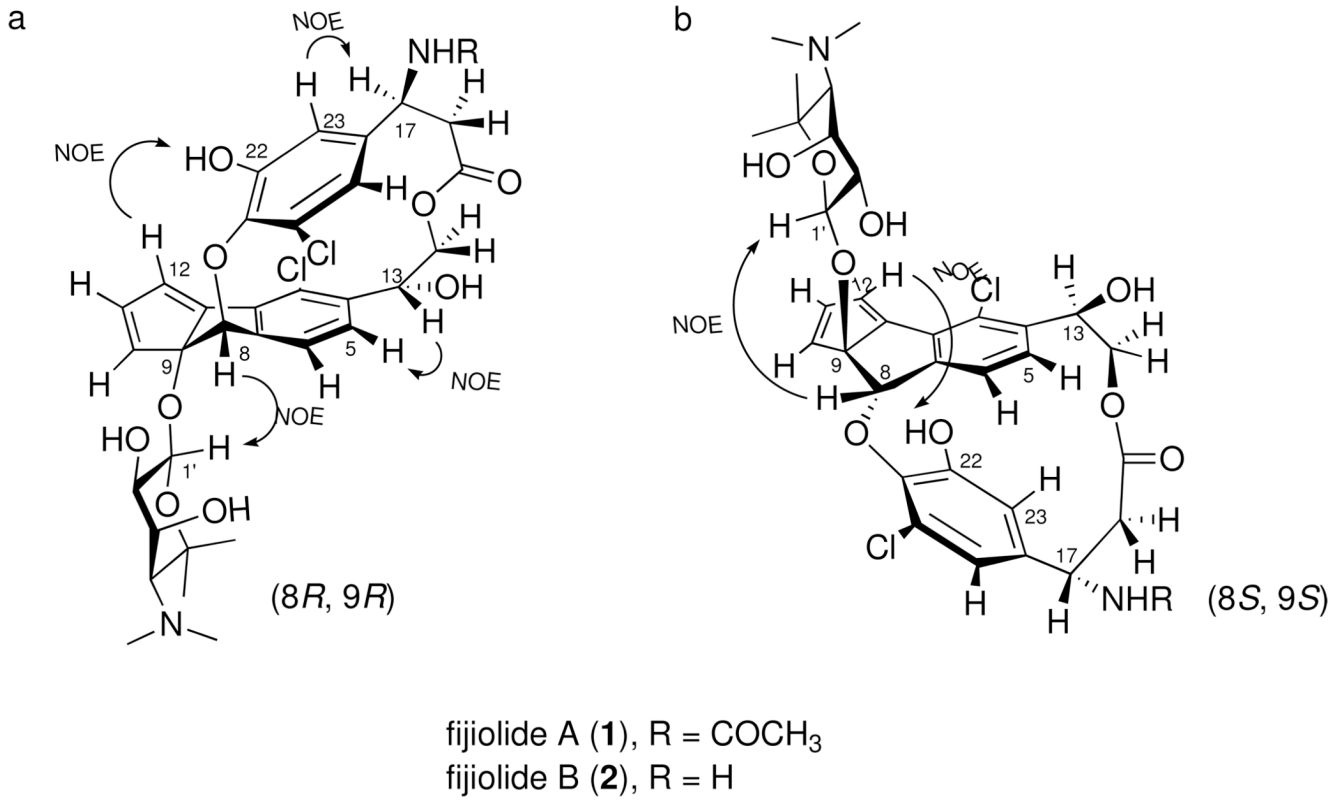

Figure 4.
The two possible stereoisomers (a, b), and selected key NOESY correlations for determination of the configurations at C-8 and C-9 for fijiolide A (a).

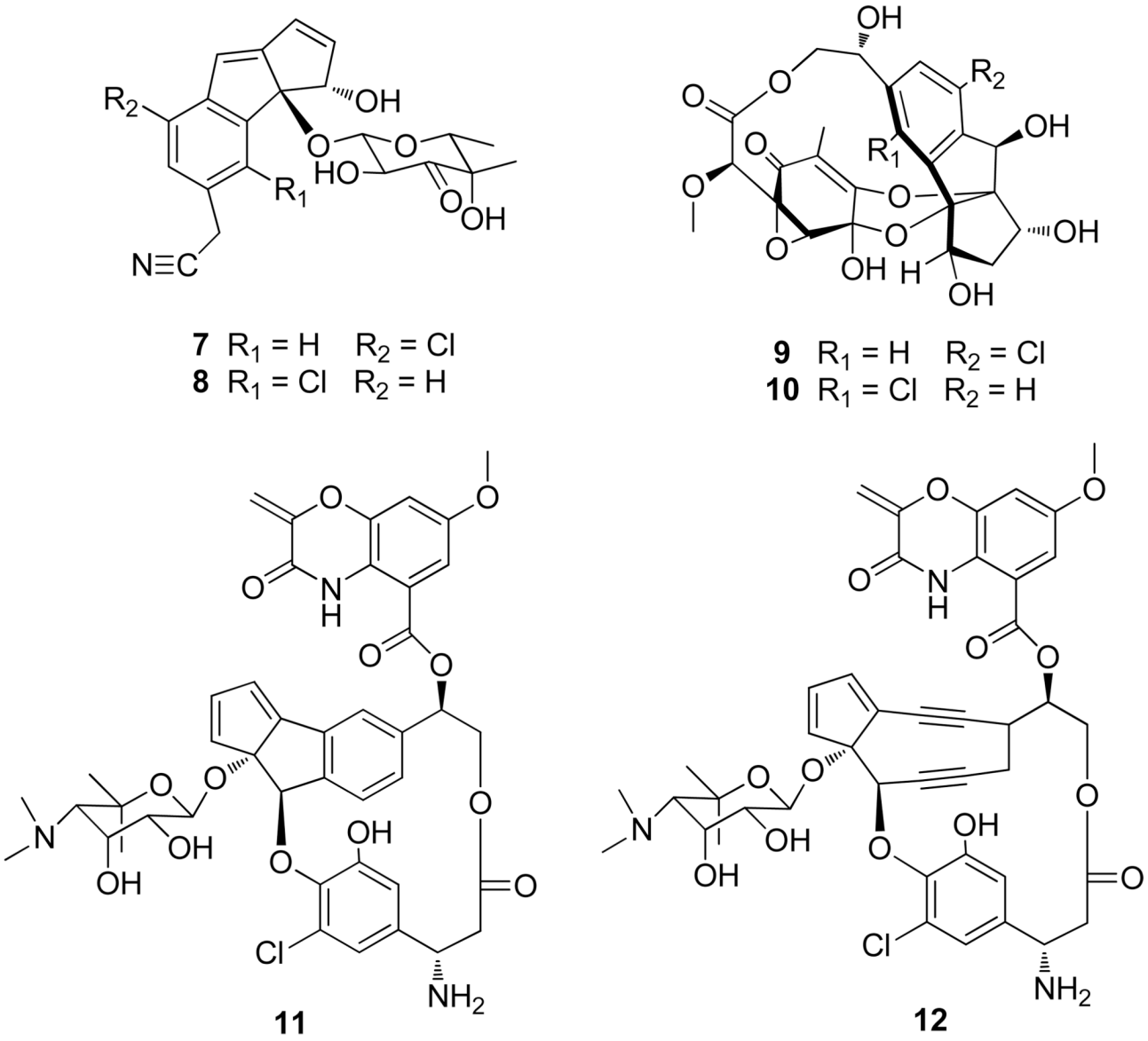

Figure 5.
Chemical structures of cyanosporasides (**7**, **8**), sporolides (**9** and **10**), aromatization product of C-1027 (**11**) and C-1027 (**12**).

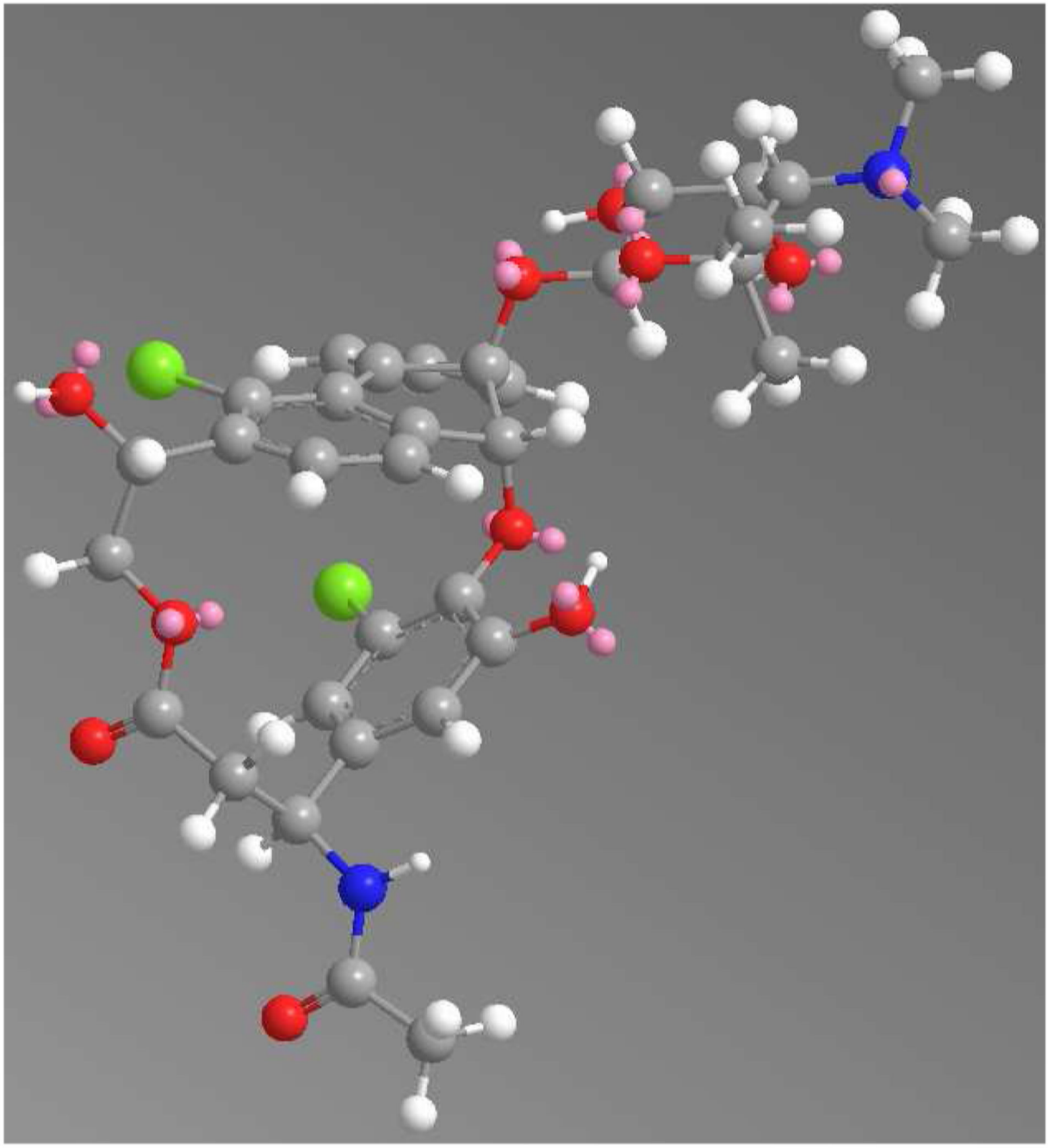

Figure 6.
Energy minimized model of fijiolide A (**1**) (calculated by ChemBio 3D (ver. 11.0), red = oxygen, green = chlorine, white = hydrogen, blue = nitrogen, grey = carbon atom).

Scheme 1.
Production of acetonide **5** from fijiolide A (**1**)

Table 1

NMR Spectroscopic Data for Fijiolide A (1) (DMSO-d_6)[a]

No.	δ_C, mult.[b]	δ_H (*J* in Hz)	COSY	HMBC[c]
1	148.8, C			
2	135.7, C			
3	126.7, C			
4	139.3, C			
5	129.1, CH	6.64, d (8.0)	6	3, 4, 6, 7, 13
6	125.3, CH	7.08, d (8.0)	5	2, 4, 5, 7, 8
7	147.7, C			
8	83.2, CH	5.87, s		1, 2, 6, 7, 9, 10, 21
9	99.8, C			
10	135.5, CH	6.62, d (5.3)	11	1, 8, 9, 11, 12
11	138.0, CH	6.65, dd (5.3, 2.1)	10, 12	1, 9, 10, 12,
12	129.4, CH	6.76, d (2.1)	11	1, 2, 9, 10, 11
13	73.1, CH	4.66, dd (11.0, 4.0)	14, 13-OH	3, 4, 5, 14
14	65.9, CH_2	4.23, dd (11.0, 4.0), 3.64, dd (11.0, 4.0)	13	4, 13, 15
15	170.0, C			
16	42.9, CH_2	2.57, dd (13.4, 3.8), 2.07, t (13.4)	17	15, 17, 18
17	49.0, CH	4.61, ddd (13.4, 13.4, 3.8)	16, 17-NH	15, 16, 18, 19, 23, 24
18	138.8, C			
19	114.2, CH	6.52, d (2.0)	23	17, 18, 20, 21, 23
20	129.2, C			
21	138.3, C			
22	151.0, C			
23	113.9, CH	5.98, d (2.0)	19	17, 18, 21, 22
24	168.4, C			
25	22.6, CH_3	1.70, s		24
1′	93.1, CH	4.45, d (8.0)	2′	9, 2′, 3′, 5′
2′	69.6, CH	2.92, dd (8.0, 3.4)	1′, 3′	1′, 4′
3′	67.5, CH	4.06, dd (8.0, 3.4)	2′, 4′	1′, 5′
4′	69.6, CH	2.98[d]		
5′	75.0, C			
4′-NMe_2	42.9, CH_3	2.79, br s		4′
4′-NMe_2	44.4, CH_3	2.79, br s		4′
6′-Meα	31.5, CH_3	1.43, s		4′, 5′, 6′-Meβ
6′-Meβ	20.6, CH_3	1.46, s		4′, 5′, 6′-Meα
13-OH		5.86	13	
17-NH		8.41, d (8.0)		16, 17, 24
22-OH		8.45, s		21, 22, 23
2′-OH		4.95, br s	2′	

No.	δ_C, mult. *b*	δ_H (*J* in Hz)	COSY	HMBC*c*
3′-OH		5.73, br s	3′	
4′-NH^+		9.09, br s	4′-NMe_2	

*a*600 MHz for ^{1}H NMR and 150 MHz for ^{13}C NMR.

*b*Numbers of attached protons were determined by analysis of 2D spectra.

*c*HMBC correlations are from the stated protons to the indicated carbons.

*d*The coupling constant could not be determined because of overlapping signals.

Table 2

NMR Spectroscopic Data for Fijiolide B (2) (DMSO-d_6)[a]

No.	δ_C, mult.[b]	δ_H (*J* in Hz)	COSY	HMBC[c]
1	148.2, C			
2	135.7, C			
3	126.9, C			
4	139.8, C			
5	129.5, CH	6.66, d (8.0)	6	3, 4, 6, 7, 13
6	125.5, CH	7.16, d (8.0)	5	2, 4, 5, 7, 8
7	147.8, C			
8	83.9, CH	5.88, s		1, 2, 6, 7, 9, 10, 21
9	100.4, C			
10	135.8, CH	6.62, d (5.3)	11	1, 8, 9, 11, 12
11	138.5, CH	6.65, dd (5.3, 2.1)	10, 12	1, 9, 10, 12,
12	129.9, CH	6.75, d (2.1)	11	1, 2, 9, 10, 11
13	72.7, CH	4.66, dd (11.0, 4.0)	14, 13-OH	3, 4, 5, 14
14	65.5, CH_2	4.28, dd (11.0, 4.0), 3.68, dd (11.0, 4.0)	13	4, 13, 15
15	168.4, C			
16	41.7, CH_2	2.85, dd (13.4, 1.8), 2.20, t (13.4)	17	15, 17, 18
17	51.2, CH	4.09, dd (13.4, 1.8)	16	15, 16, 18, 19, 23
18	133.1, C			
19	114.4, CH	6.76, d (2.0)	23	17, 18, 20, 21, 23
20	130.1, C			
21	139.9, C			
22	151.7, C			
23	115.2, CH	6.06, d (2.0)	19	17, 18, 21, 22
1′	93.4, CH	4.44, d (8.0)	2′	9, 2′, 3′, 5′
2′	69.6, CH	2.91, br s	1′, 3′	1′, 4′
3′	67.8, CH	4.05, br s	2′, 4′	1′, 5′
4′	69.6, CH	2.99, br s	3′	4′-NMe_2
5′	75.3, C			
4′-NMe_2	42.9, CH_3	2.79, br s		4′
4′-NMe_2	44.6, CH_3	2.79, br s		4′
6′-Meα	31.9, CH_3	1.37, s		4′, 5′, 6′-Meβ
6′-Meβ	21.2, CH_3	1.41, s		4′, 5′, 6′-Meα
13-OH		5.86	13	
17-NH_2		8.58		
22-OH		8.84, s		21, 22, 23
2′-OH		4.97, br s	2′	
3′-OH		5.72, br s	3′	
4′-NH^+		9.13, br s	4′-NMe_2	

[a] 600 MHz for ^{1}H NMR.

[b] Numbers of attached protons were determined by analysis of 2D spectra.

[c] HMBC correlations are from the stated protons to the indicated carbons.